# We are IntechOpen,
the world's leading publisher of
Open Access books
Built by scientists, for scientists

## 4,800
Open access books available

## 122,000
International authors and editors

## 135M
Downloads

## 154
Countries delivered to

Our authors are among the

## TOP 1%
most cited scientists

## 12.2%
Contributors from top 500 universities

CLARIVATE ANALYTICS
BOOK CITATION INDEX
INDEXED

**WEB OF SCIENCE**™

Selection of our books indexed in the Book Citation Index
in Web of Science™ Core Collection (BKCI)

## Interested in publishing with us?
Contact book.department@intechopen.com

Numbers displayed above are based on latest data collected.
For more information visit www.intechopen.com

# Titanium Dioxide Films for Photocatalytic Degradation of Methyl Orange Dye

Rodrigo Teixeira Bento and Marina Fuser Pillis

Additional information is available at the end of the chapter

## Abstract

The aim of this work was to characterize and evaluate the influence of the thickness on the photocatalytic efficiency of titanium dioxide thin films on the degradation of methyl orange dye under UV light irradiation. The films of 280 and 468 nm thick were deposited on borosilicate substrates at 400°C by the MOCVD technique using titanium isoproxide IV as precursor. XRD analyses showed the formation of anatase-$TiO_2$ phase. Cross-sectional FE-SEM images show that the films presented a dense columnar structure and grown perpendicularly to the substrate surface. The photocatalytic activity of the catalysts was studied using UV-vis spectrophotometry The $TiO_2$ film with 468 nm of thickness presented higher photocatalytic activity exhibiting 69% of dye degradation. The increase of grain size and thickness of the films promoted an improvement of photocatalytic efficiency.

**Keywords:** $TiO_2$ films, MOCVD, photocatalytic activity

## 1. Introduction

The availability of water is of great importance for the development of economic activities and mainly for human health. However, the rapid increase in industrial production resulted in serious consequences to the environment by generating waste and contaminating the water reserves [1–3]. The pharmaceutical products, pesticides, azo dyes, herbicides, and hormones are the main contaminants in water [4–6]. The textile activities are responsible for 15% of the industrial consumption of water [7]. It is estimated that approximately 15–20% of the chemical species, including dyes, are disposed of as effluent after processing [8].

Among the more than 10,000 types of dyes available [9], the azo compounds stand out and are characterized by the presence of one or more chromophore groups (—N=N—) in their chemical structure [10–12]. The intensity of absorption and also the shades of color vary according to the other electrons $\pi$ and $n$ which are in conjunction [13]. An example of azo dye is the methyl orange (MO).

Methyl orange dye ($C_{14}H_{14}N_3NaO_3S^-Na^+$) is a compound generally used as acid-base indicator [14]. Sha et al. [14] shows that a decrease in pH causes a shift in the absorption band of MO, and a change in its coloration occur, being orange in basic pH and red in acidic condition [15]. The MO structure is characterized by the azo group among the aromatic rings [15, 16] and is shown schematically in **Figure 1**.

Several researches have been done to develop new technologies to remove dyes and others pollutants from wastewater effluent. Hassan et al. [17] studied the use of heterogeneous photocatalysis for the treatment of landfill leachate, comparing the efficiency of this technique to other methods, besides the parameters that influence the process results. The study revealed to be possible to remove pollutants found in landfill leachate using $TiO_2$ as catalyst. The best photocatalytic results were obtained for anatase and anatase-rutile mixture. Jorfi et al. [18] developed $TiO_2$ catalyst supported on magnetic activated carbon for the oxidative degradation of benzotriazole (BTA) by UV-Fenton process. According to the authors, the catalyst showed good reusability, since after five cycles of reuse, the efficiency in the degradation of BTA dropped from 92.2 to 71.6%. Konstantinou and Albanis [19] and Sleiman et al. [20] evaluated the photocatalytic degradation of azo dyes by photocatalytic oxidation using $TiO_2$ under UV-vis irradiation. Both works state the efficiency of the heterogeneous photocatalysis method in water treatment. Akrout and Bousselmi [21] carried out the electrochemical degradation of synthetic wastewater containing biazo dye on boron-doped diamond anode (BDD) at current densities from 8 to 48 $Am^{-2}$. The authors verified the influence of pH and of the applied current density on degradation. The decrease of pH and the increase of current density showed a positive effect on the oxidation. Vallejo et al. [22] presented a review about the capacity for polychlorinated dibenzo-p-dioxins and dibenzofurans (PCDD/Fs) remediation by means of Advanced Oxidation Processes.

Advanced Oxidation Processes (AOPs) are the most attractive methods used to degrade polluting compounds based on the use of highly oxidizing species to promote greater efficiency in the treatment process [23].

AOPs are characterized by generating free radicals, especially the hydroxyl radical ($OH^\bullet$), transforming the organic contaminants in simpler species, such as carbon dioxide, water, and inorganic anions [24]. Hydroxyl radicals can be generated from reactions involving ozone ($O_3$) and hydrogen
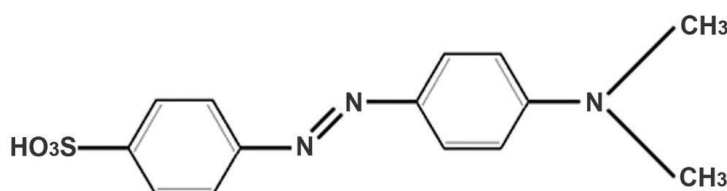


**Figure 1.** Structure of the methyl orange dye molecule.

peroxide ($H_2O_2$)—oxidants with high degrading power—semiconductors such as titanium dioxide ($TiO_2$) and ultraviolet irradiation (UV) [25, 26]. **Figure 2** presents the main techniques of AOP [22].

The first studies in photocatalysis were developed by Fukushima and Honda [27], when they observed that $TiO_2$ exposed to the sunlight could produce the photocatalytic dissociation of water, producing hydrogen. Recent researches deal with heterogeneous photocatalysis for applications in water treatment [2, 6, 23, 26]. **Figure 3** shows the schematic diagram of photocatalytic process, showing the photoactivation of a catalyst semiconductor and the production of oxidizing radicals. This process is based on the electronic excitation of certain semiconducting oxides (catalyst) by means of radiant energy—visible or UV light [28, 29]. The reaction is activated by absorption of a photon with energy equal or higher than the bandgap energy ($E_{bg}$) of the catalyst [5]. When an electron is promoted from the valence band (VB) to the conduction band (CB), a hole (h+) is generated in the VB (Eq. (1)). The electrons transferred to CB are responsible for reduction reactions, producing gaseous hydrogen and other oxidizing species (Eqs. (2) and (3)). The holes react with the adsorbed water molecules on the surface of the photocatalyst to generate $OH^\bullet$ radicals (Eqs. (4) and (5)), allowing the oxidation of organic molecules and ionized species [5, 6].
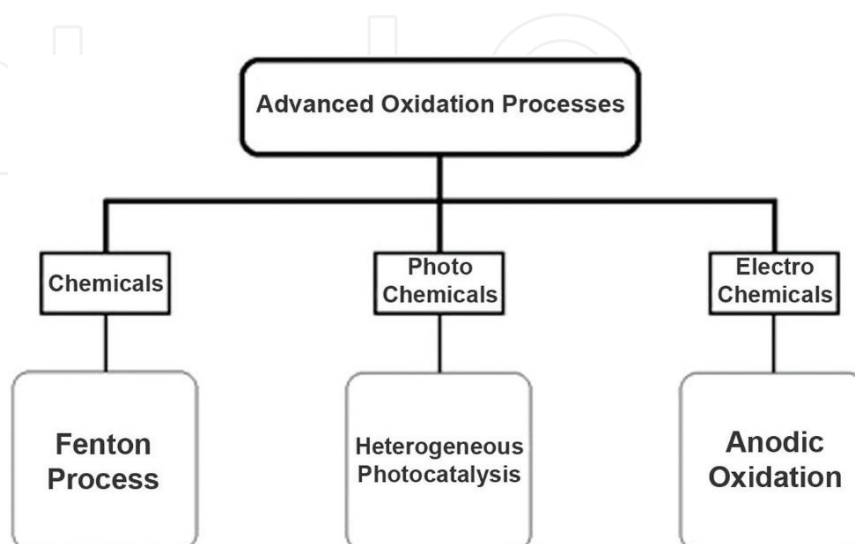
$$Photocatalyst + h\upsilon \;\rightarrow\; Photocatalyst\!\left(e_{cb}^- + h_{vb}^+\right) \tag{1}$$

$$Photocatalyst\!\left(e_{cb}^-\right) + 2H_{(ads)}^+ \;\rightarrow\; H_2 \tag{2}$$

$$Photocatalyst\!\left(e_{cb}^-\right) + H_2O_{(ads)} \;\rightarrow\; H^+ + OH \tag{3}$$

$$Photocatalyst\!\left(h_{vb}^+\right) + H_2O_{(ads)} \;\rightarrow\; H^+ + OH^\bullet \tag{4}$$

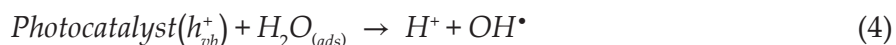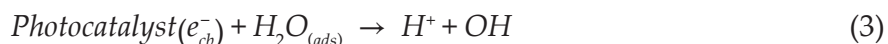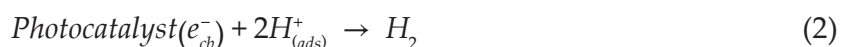$$Photocatalyst\!\left(h_{vb}^+\right) + OH_{(ads)}^- \;\rightarrow\; OH^\bullet \tag{5}$$
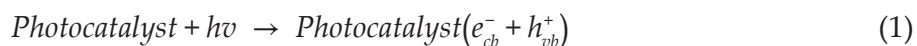


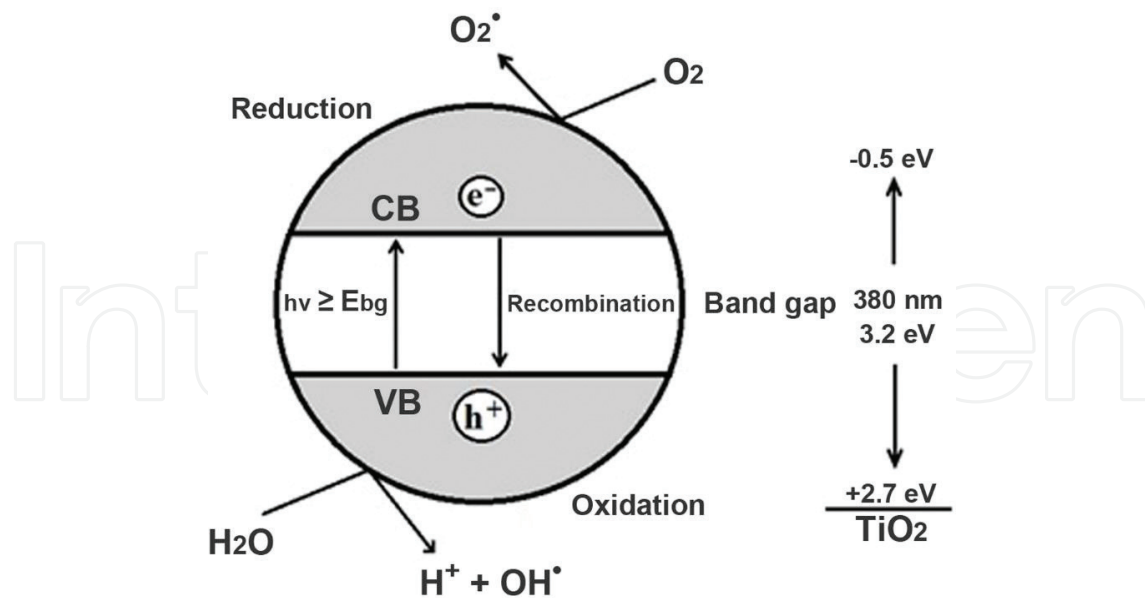**Figure 2.** Principal advanced oxidation processes.

**Figure 3.** Schematic diagram of photocatalytic process and bandgap of TiO$_2$ semiconductor.

The main factors that influence the photocatalytic degradation are pH, initial concentration of dyes, reaction temperature, catalyst concentration, oxidizing agents, light intensity, and irradiation time [6, 17, 20]. Acid pH is more favorable for photocatalytic applications than neutral or alkaline pH [30]. Chanathaworn et al. [31] studied the effects of irradiation intensity of black light lamp on the degradation of the Rhodamine B. According to the results, an increase in the irradiation intensity intensified the dye degradation.

Titanium dioxide (TiO$_2$) is the most crystalline semiconductor used in photocatalytic process [26, 32]. It presents three polymorphic phases: anatase and rutile, with tetragonal structure; and brookite, orthorhombic [33, 34], being anatase the phase of greater degradative efficiency [17]. Due to the TiO$_2$ bandgap energy being relatively wide (E$_g$ = 3.2 eV for anatase; E$_g$ = 3.0 eV for rutile; E$_g$ = 3.1 eV for brookite) [6, 33, 34], the material can only be activated by UV irradiation with $\lambda$ < 380 nm [35].

Absalan et al. [36] developed TiO$_2$ nanoparticles in anatase, rutile, and brookite phases by sol-gel method using different calcination temperature and time and doped by transition metals (cadmium, chromium, nickel, manganese, iron, and cobalt). According to the authors, the proportion of anatase phase increased after doping process, besides improving the photocatalytic efficiency. According to Carp et al. [37], the doping process reduces the bandgap, making the material active in the region of the visible spectrum of light.

Among several techniques used on the synthesis of TiO$_2$ [38–41], the chemical vapor deposition (CVD) is widely employed [42]. Pierson [43] defines CVD as the deposition of a solid on a heated surface from a chemical reaction in the vapor phase. In this process, the vapor of a volatile compound reacts near or over the surface to be coated (substrate), forming a solid deposit by nucleation of the chemical element that composes the material to be deposited, from a movement governed by processes of diffusion and convection of matter [43].

The crystalline structure, grain size, and, mainly, the chemical composition and the thickness of the films are essential parameters to define its properties and applications [44]. The present research aims the structural and morphological characterization of $TiO_2$ thin films grown at 400°C by MOCVD process and to study the influence of the thickness on the photocatalytic efficiency to degrade methyl orange dye under UV light.

# 2. Experimental procedure

The growth of $TiO_2$ thin films was realized by metalorganic chemical vapor deposition (MOCVD) in a conventional horizontal reactor at 400°C under a pressure of 50 mbar. Titanium(IV) isopropoxide (*Sigma-Aldrich*, 99.999%) was used as precursor of titanium and oxygen. Nitrogen (flow rate of 0.5 mL min$^{-1}$) was used as carrier and purge gas. The borosilicate substrates (25 × 76 × 1 mm) were previously cleaned in a 5% $H_2SO_4$ aqueous solution, rinsed in deionized water, dried in nitrogen, and immediately inserted into the reactor. **Figure 4** shows schematically the MOCVD equipment [45]. The main components are the reaction chamber, which consists of a quartz tube heated by an infrared oven containing the sample holder, and a vacuum pump that keeps the reaction chamber under a pressure below the atmospheric. The TTiP is maintained in a bubbler heated to 39°C. The gas conduction lines are made of stainless steel and are kept heated to prevent condensation and premature pyrolysis of the precursor.

## 2.1. Characterization of the films

X-ray diffraction (XRD) diagrams, obtained in a *Rigaku Multiflex* equipment using CuK$\alpha$ radiation ($\lambda$ = 1.54148 Å), incidence angle of 2.5°, and scan rate of 0.02°, were used to identify the phases formed. Measurements of surface roughness and mean grain size were performed by atomic force microscopy (AFM) operating in the Tapping mode (*SPM Bruker NanoScope IIIA*), employing a silicon tip with a curvature radius of 15 nm. The thickness of the films was measured in the cross section of the samples by using a field emission scanning electron microscope (FE-SEM) *JSM6701F* X-ray photoelectron spectroscopy (XPS) measurements with spot size beam of 400 μm were conducted in order to determine the chemical state of
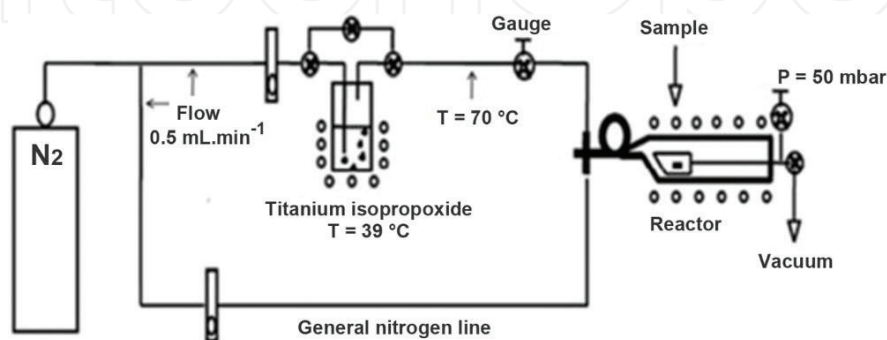


**Figure 4.** MOCVD equipment shown schematically (adapted from reference 45).
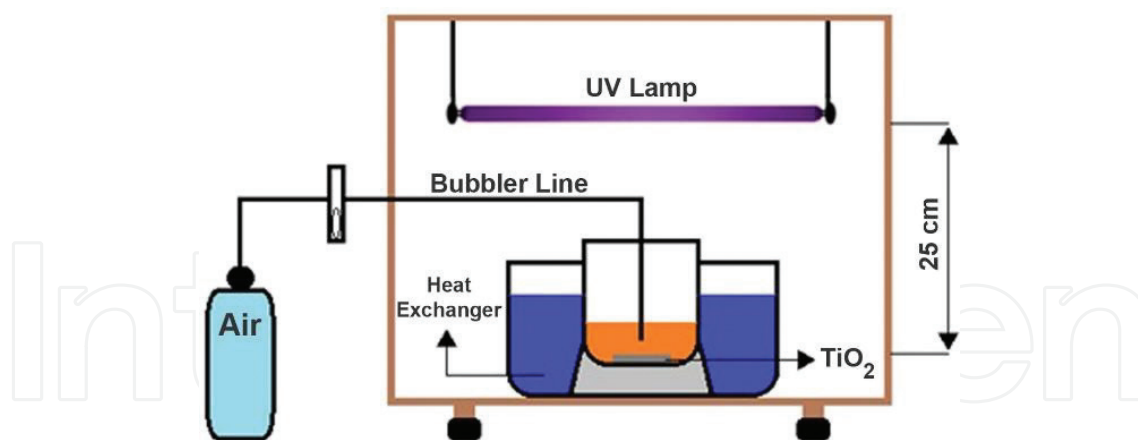
**Figure 5.** Schematic diagram of the photocatalytic reactor.

the species near the solid surface. A *Thermo Scientific, K-Alpha model* equipment was used. After the acquisition of the high-resolution spectra, the deconvolution was done using the algorithm Smart in the software Avantage®. The binding energies were corrected considering the C1s reference peak at 214.8 eV.

## 2.2. Photocatalytic tests

The photocatalytic activities of the $TiO_2$ films were estimated by measuring the degradation of methyl orange dye (MO, 5 mg $L^{-1}$) in an aqueous solution (pH = 2), under UV light irradiation (Sankyo Denki Co., Ltd., 15 W, $\lambda$ = 352 nm). The changes in the MO concentration were monitored using a UV-vis spectrophotometer (*Global Trade Technology*). For this purpose, the films were placed in a reactor (**Figure 5**) containing 40 mL of the dye solution and were illuminated by two tubular UV lamps for 300 min. Synthetic air ($N_2$/20 wt.% $O_2$) was bubbled into the solution during the tests.

The photocatalytic reactor consists of a glass chamber containing the MO dye solution to be degraded, the $TiO_2$ catalyst supported in borosilicate, and the source of radiation. The components of the photoreactor were arranged in a box to prevent loss of photons and to protect users against the emitted UV radiation. The distance between the photocatalyst and the UV lamps was set at 25 cm.

## 3. Results and discussion

The cross section of the samples was observed and the thickness of the $TiO_2$ films grown on borosilicate was measured. **Figure 6a** shows the FE-SEM image of the 280 nm thick film, revealing the formation of a dense film. The AFM image (**Figure 7a**) shows that the film presents homogeneous morphology, composed of rounded grains of 124 nm mean size and of 19 nm RMS roughness, which can be considered favorable for photocatalytic applications [37], since it facilitates the contact of the adsorbed substances with the film, increasing its photocatalytic efficiency [46].
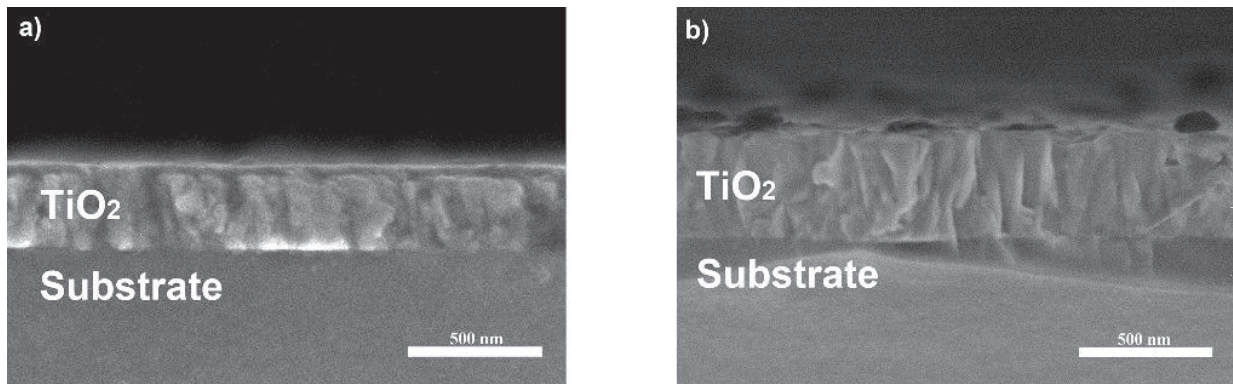
**Figure 6.** FE-SEM fracture images for TiO$_2$ films: (a) thickness of 280 nm and (b) thickness of 468 nm.
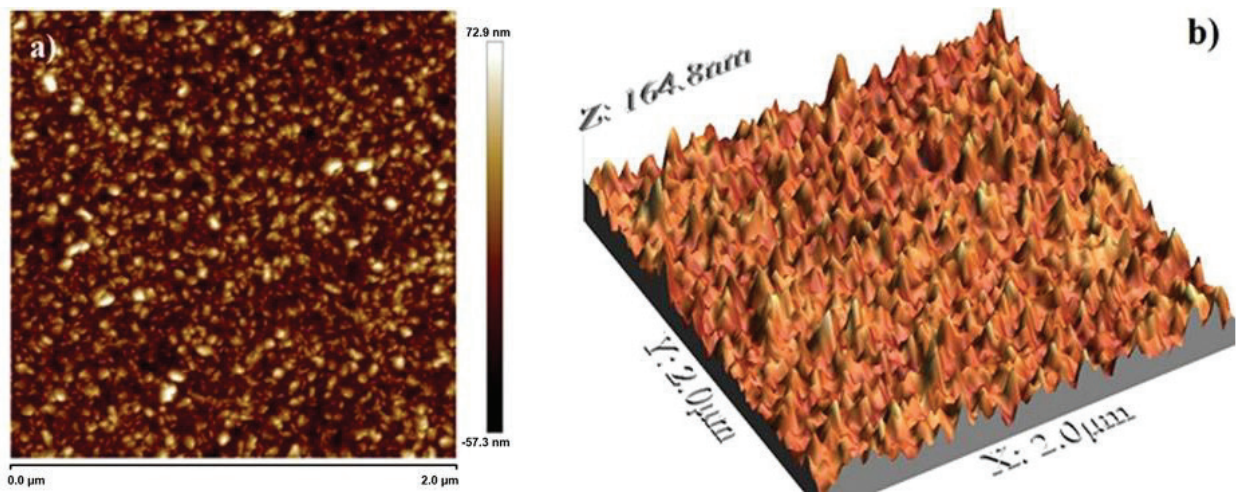


**Figure 7.** AFM images of TiO$_2$ film with thickness of 280 nm: (a) topography and (b) 3D image.

The RMS (*Root Mean Square*) roughness expresses the values of a roughness profile that moves away from the midline, in other words, it is the standard deviation of the mean height $Z$ [47], being mathematically expressed as:

$$RMS = \sqrt{\frac{\sum_{N=1}^{N}(Z_N - Z)^2}{N-1}} \qquad (6)$$

where $N$ is the number of peaks; $Z_N$ is the height of each peak; and $Z$ is the mean height of $N$ peaks.

The morphology of the surface of the TiO$_2$ film grown with thickness of 468 nm (**Figure 8a**) presents a mean grain size of 214 nm and roughness values of the order of 16 nm (**Table 1**). It can be observed as a dense film with columnar structure (**Figure 6b**). Results presented by Krumdieck et al. [48] showed that the increase of the thickness of the films caused a decreased of the roughness, similar trend with the values exhibited in the present work. The results clearly show that the increase of the growth time (**Table 1**) caused an increase in the film thickness, as evidenced by Antunes et al. [49].
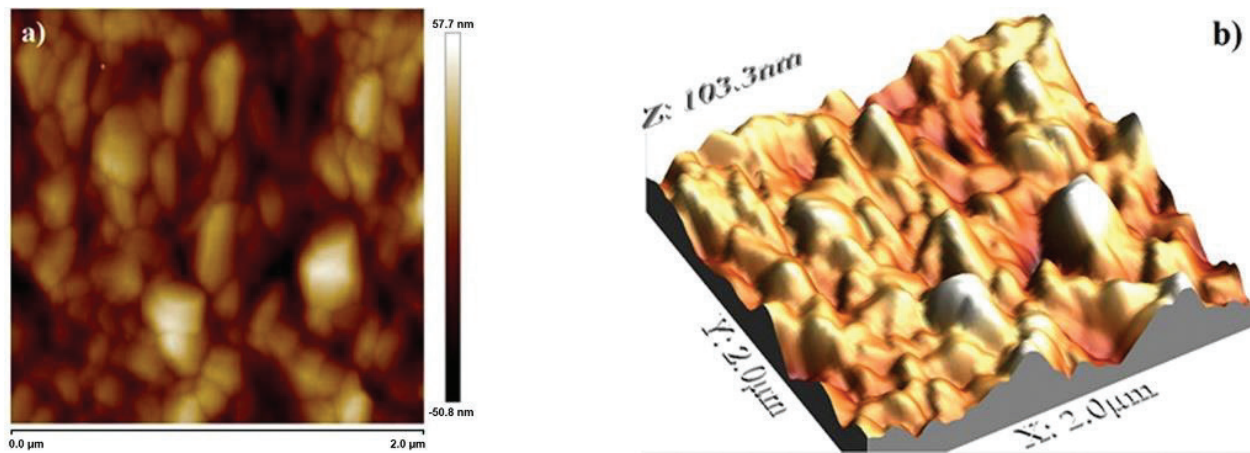
**Figure 8.** AFM images of TiO$_2$ film with thickness of 468 nm: (a) topography and (b) 3D image.

| Temperature of deposition [°C] | Growth time [min] | Film thickness [nm] | Mean grain size [nm] | RMS roughness [nm] |
|---|---|---|---|---|
| 400 | 30 | 280 | 124 | 19 |
| 400 | 40 | 468 | 214 | 16 |

**Table 1.** Characteristics of TiO$_2$ films grown by MOCVD on borosilicate.

**Figure 9** shows the XRD patterns of TiO$_2$ films grown at 400°C with different thickness. The characteristic peaks correspond to the crystalline anatase phase (JCPDS 21–1272).

**Figure 10** shows the XPS spectra of the 280 nm TiO$_2$ thin film. The surface of the films contains high quantities of Ti and O elements and C (**Figure 10a**). According to Liu et al. [50] and Babelon et al. [51], the presence of C1s peak was ascribed to the residual carbon from the metalorganic precursor and to surface pollution provoked for the sample exposition to air before the XPS experiments. Ti2p spectrum (**Figure 10b**) appeared at 459.5 and 465.2 eV attributed, respectively, to Ti2p$_{3/2}$ and Ti2p$_{1/2}$ peaks of O—Ti—O in TiO$_2$ [50, 52]. Bharti et al. [53] and Lin et al. [54] suggested that these peaks are consistent with Ti$^{4+}$ in TiO$_2$ lattice. The O1s spectrum (**Figure 10c**) reveals two peaks at 530.7 and 532.4 eV. The first one can be attributed to the oxygen present in the TiO$_2$ lattice, and the other one represents the surface oxygen [52].

**Figure 11** exhibits the C/C$_0$ graphs as a function of the time of exposure to UV radiation, where C represents the dye concentration at each time interval and C$_0$ is the initial concentration. The photolysis curve demonstrates that without the presence of the catalyst (TiO$_2$ film) there was no degradation of the dye. The TiO$_2$ film with thickness of 280 nm degraded 28% of MO dye for a total test time of 300 minutes while the TiO$_2$ film with 468 nm of thickness, showed 69% of dye degradation in the same condition, that is, it was approximately 2.5× more efficient.

A large surface area is necessary for the light irradiation and the photocatalyst contacting with pollutant compound and, consequently, the photocatalysis efficiency of the TiO$_2$ films
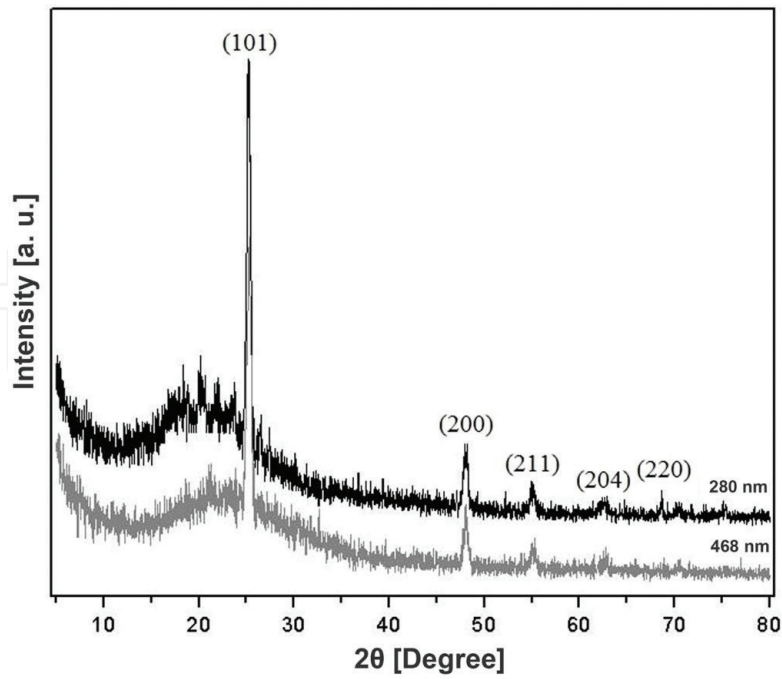
**Figure 9.** XRD patterns of the TiO₂ films grown on borosilicate at 400°C.
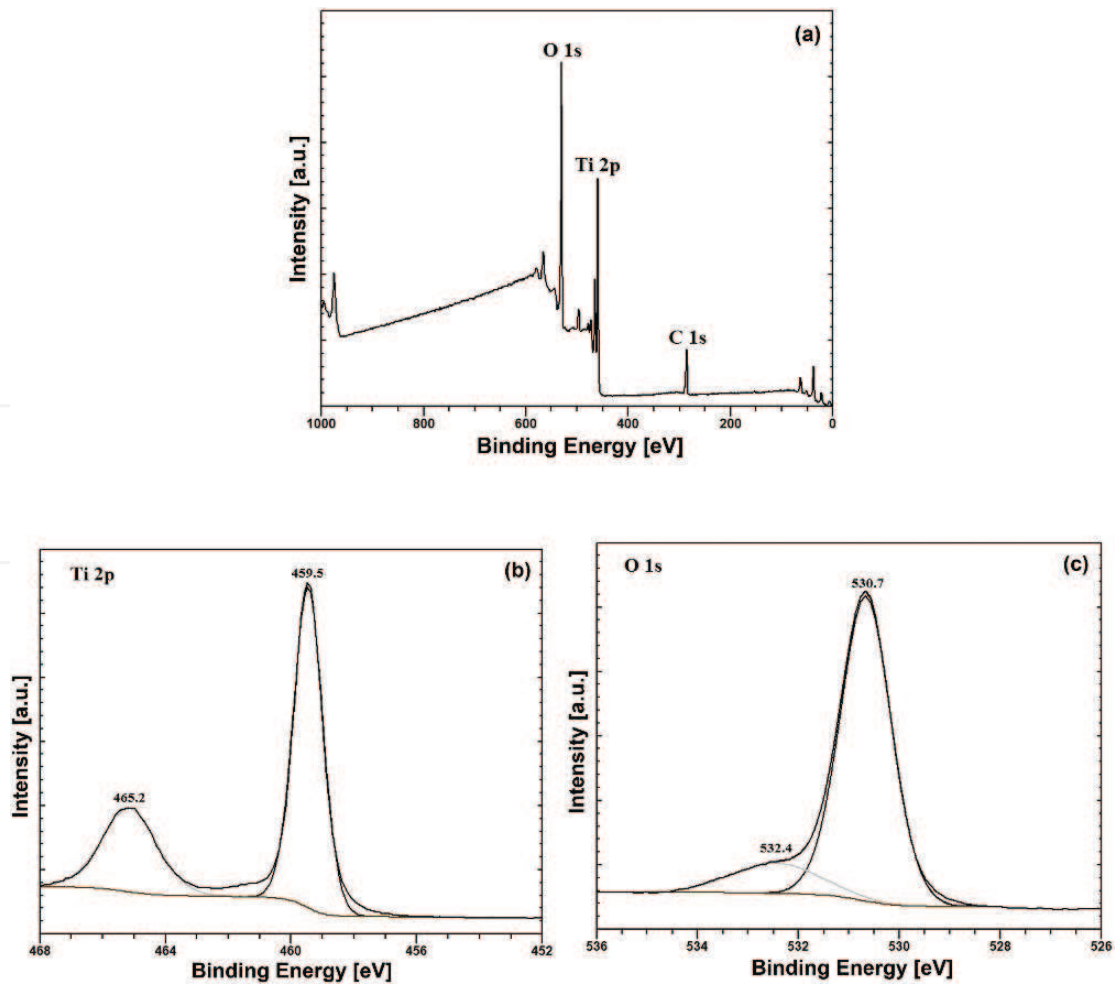


**Figure 10.** XPS spectra of the 280 nm TiO₂ films (a) survey; (b) Ti2p, and (c) O1s.
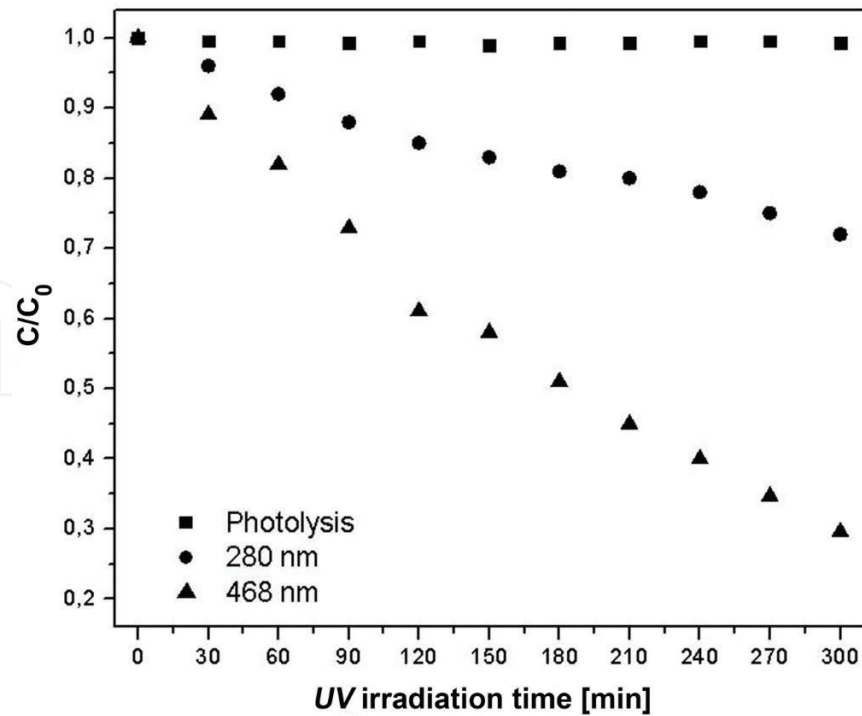
**Figure 11.** MO dye concentration as a function of the time of exposure to UV irradiation ($\lambda$ = 352 nm) with and without the presence of TiO$_2$ films grown by MOCVD.

is intensified [55, 56]. The increase in thickness is also favorable for the photocatalytic performance, since thinner films have a higher electron recombination rate than thicker films [57].

## 4. Conclusions

TiO$_2$ films grown by MOCVD process were demonstrated to be effective for methyl orange dye degradation under UV irradiation. The films presented the formation of anatase phase, and surface morphology composed of rounded grains. The methyl orange dye does not degrade under UV radiation without the presence of the TiO$_2$ photocatalyst. The best photocatalytic result occurred for the film with thickness of 468 nm, which exhibited 69% of dye degradation in 300 minutes. The results suggest that the morphology and structural characteristics influence the photocatalytic activity of the TiO$_2$ films.

## Conflict of interest

The authors declare that there is no conflict of interest regarding the publication of this chapter.

## Author details

Rodrigo Teixeira Bento and Marina Fuser Pillis*

*Address all correspondence to: mfpillis@ipen.br

Materials Science and Technology Center, Nuclear and Energy Research Institute
(CCTM-IPEN/CNEN), Cidade Universitária, São Paulo, Brazil

## References

[1] Khaoulani S, Chaker H, Cadet C, Bychkov E, Cherif L, Bengueddach A, Fourmentin S. Wastewater treatment by cyclodextrin polymers and noble metal/mesoporous $TiO_2$ photocatalysts. Comptes Rendus Chimie. 2015;**18**:23-31

[2] Tsoumachidou S, Lambropoulou D, Poulios I. Homogeneous photocatalytic oxidation of UV filter paraaminobenzoic acid in aqueous solutions. Environmental Science and Pollution Research. 2017;**24**:1113-1121

[3] Josephine GAS, Nisha UM, Meenakshi G, Sivasamy A. Nanocrystalline semiconductor doped rare earth oxide for the photocatalytic degradation studies on acid blue 113: A di-azo compound under UV slurry photoreactor. Ecotoxicology and Environmental Safety. 2015;**121**:67-72

[4] Horáková M, Klementová S, Kriz P, Balakrishna SK, Spatenka P, Golovko O, Hájková P, Exnar P. The synergistic effect of advanced oxidation processes to eliminate resistant chemical compounds. Surface & Coatings Technology. 2014;**241**:154-158

[5] Akpan UG, Hameed BH. Parameters affecting the photocatalytic degradation of dyes using $TiO_2$-based photocatalysts: A review. Journal of Hazardous Materials. 2009; **170**:520-529

[6] Reza KM, Kurny ASW, Gulshan F. Parameters affecting the photocatalytic degradation of dyes using $TiO_2$: A review. Applied Water Science. 2017;**7**:1569-1578

[7] Silva MC, Corrêa AD, Torres JA, Amorim MTSP. Descoloração de corantes industriais e efluentes têxteis simulados por peroxidase de nabo (Brassica campestre). Química Nova. 2012;**35**:889-894

[8] Jin XC, Liu GQ, Xu ZH, Tao WY. Decolorization of a dye industry effluent by *Aspergillus fumigatus* XC6. Applied Microbiology Biotechnology. 2007;**74**:239-243

[9] Wang C, Yediler A, Linert D, Wang Z, Kettrup A. Toxicity evaluation of reactive dye-stuffs, auxiliaries and selected effluents in textile finishing industry to luminescent bacteria *Vibrio fischeri*. Chemosphere. 2002;**46**:339-344

[10] Kasic H, Bozic AL, Koprivanace N. Heterogeneous photocatalytic treatment of textile dye effluent containing Azo dye: Direct Crysophenine G. Der Chemica Sinica. 2011;**2**:37-46

[11] Saratale RG, Saratale GD, Chang JS, Govindwar SP. Bacterial decolorization and degradation of azo dyes: A review. Journal of the Taiwan Institute of Chemical Engineers. 2011;**42**:138-157

[12] Kaur N, Dhaka G, Singh J. Simple naked-eye ratiometric and colorimetric receptor for anions based on azo dye featuring with benzimidazole unit. Tetrahedron Letters. 2015; **56**:1162-1165

[13] Aljamali N. Review in azo compounds and its biological activity. Biochemistry & Analytical Biochemistry. 2015;**4**:1000169

[14] Sha Y, Mathew I, Cui Q, Clay M, Gao F, Zhang XJ, Gu Z. Rapid degradation of azo dye methyl orange using hollow cobalt nanoparticles. Chemosphere. 2016;**144**:1530-1535

[15] Guettai N, Amar HA. Photocatalytic oxidation of methyl orange in presence of titanium dioxide in aqueous suspension. Part I: Parametric study. Desalination. 2005;**185**:427-437

[16] Kaur J, Singhal S. Facile synthesis of ZnO and transition metal doped ZnO nanoparticles for the photocatalytic degradation of methyl Orange. Ceramics International. 2014;**40**:7417-7424

[17] Hassan M, Zhao Y, Xie B. Employing $TiO_2$ photocatalysis to deal with landfill leachate: Current status and development. Chemical Engineering Journal. 2016;**285**:264-275

[18] Jorfi S, Kakavandi B, Motlagh HR, Ahmadi M, Jaafarzadeh N. A novel combination of oxidative degradation for benzotriazole removal using $TiO_2$ loaded on $Fe^{II}Fe_2^{III}O_4@C$ as an efficient activator of peroxymonosulfate. Applied Catalysis B: Environmental. 2017;**219**:216-230

[19] Konstantinou IK, Albanis TA. $TiO_2$-assisted photocatalytic degradation of azo dyes in aqueous solution: Kinetic and mechanistic investigations—A review. Applied Catalysis B: Environmental. 2004;**49**:1-14

[20] Sleiman M, Vildozo D, Ferronato C, Chovelon JM. Photocatalytic degradation of azo dye Metanil Yellow: Optimization and kinetic modeling using a chemometric approach. Applied Catalysis B: Environmental. 2007;**77**:1-11

[21] Akrout H, Bousselmi L. Water treatment for color and COD removal by electrochemical oxidation on boron-doped diamond anode. Arabian Journal of Geosciences. 2012;**6**:1-9

[22] Vallejo M, Román MFSR, Ortiz I, Irabien A. Overview of the PCDD/Fs degradation potential and formation risk in the application of advanced oxidation processes (AOPs) to wastewater treatment. Chemosphere. 2015;**118**:44-56

[23] Guz R, De Moura C, Da Cunha MAA, Rodrigues MB. Factorial design application in photocatalytic wastewater degradation from TNT industry—Red water. Environmental Science Pollution Research International. 2016;**24**:6055-6060

[24] Pignatello JJ, Oliveros E, Mackay A. Advanced oxidation processes for organic contaminant destruction based on the Fenton reaction and related chemistry. Critical Reviews in Environmental Science and Technology. 2006;**36**:1-84

[25] Azbar N, Yonar T, Kestioglu K. Comparison of various advanced oxidation processes and chemical treatment methods for COD and color removal from polyester and acetate fiber dyeing effluent. Chemosphere. 2004;**55**:35-43

[26] Ângelo J, Magalhães P, Andrade L, Mendes A. Characterization of $TiO_2$-based semiconductors for photocatalysis by electrochemical impedance spectroscopy. Applied Surface Science. 2016;**387**:183-189

[27] Fujishima A, Honda K. Electrochemical photolysis of water at a semiconductor electrode. Nature. 1972;**238**:37-38

[28] Athalathil S, Erjavec B, Kaplan R, Stuber F, Bengoa C, Font J, Fortuny A, Pintar A, Fabregat A. $TiO_2$-sludge carbon enhanced catalytic oxidative reaction in environmental wastewaters applications. Journal of Hazardous Materials. 2015;**300**:406-414

[29] Gomes O Jr, Borges Neto W, Machado AEH, Daniel D, Trovó AG. Optimization of fipronil degradation by heterogeneous photocatalysis: Identification of transformation products and toxicity assessment. Water Research. 2017;**110**:133-140

[30] Shao C, Zhou G, Li Z, Wu Y, Xu D, Sun B. Fabrication of large-diameter tube-like mesoporous $TiO_2$ via homogeneous precipitation and photocatalytic decomposition of papermaking wastewater. Chemical Engineering Journal. 2013;**230**:227-235

[31] Chanathaworn J, Bunyakan C, Wiyaratn W, Chungsiriporn J. Photocatalytic decolorization of basic dye by $TiO_2$ nanoparticle in photoreactor. Songklanakarin Journal of Science & Technology. 2012;**34**:203-210

[32] Zhao F, Dong B, Gao R, Su G, Liu W, Shi L, Xia C, Cao L. A three-dimensional graphene-$TiO_2$ nanotube nanocomposite with exceptional photocatalytic activity for dye degradation. Applied Surface Science. 2015;**351**:303-308

[33] Hanaor DAH, Sorrell CC. Review of the anatase to rutile phase transformation. Journal of Materials Science. 2011;**46**:855-874

[34] Guo T-L, Li J-G, Sun X, Sakka Y. Photocatalytic growth of Ag nanocrystals on hydrothermally synthesized multiphasic $TiO_2$/reduced graphene oxide (rGO) nanocomposites and their SERS performance. Applied Surface Science. 2017;**423**:1-12

[35] Dhayal M, Kapoor R, Sistla PG, Pandey RR, Kar S, Saini KK, Pande G. Strategies to prepare $TiO_2$ thin films, doped with transition metal ions, that exhibit specific physicochemical properties to support osteoblast cell adhesion and proliferation. Materials Science and Engineering. C. 2014;**37**:99-107

[36] Absalan Y, Bratchikova IG, Lobanov NN, Kovalchukova OV. Novel synthesis method for photo-catalytic system based on some 3d-metal titanates. Journal of Materials Science: Materials in Electronics. 2017;**28**:18207-18219

[37] Carp O, Huisman CL, Reller A. Photoinduced reactivity of titanium. Progress in Solid State Chemistry. 2004;**32**:33-177

[38] El-Sheikh SM, Khedra TM, Hakkib A, Ismaila AA, Badawy WA, Bahnemann DW. Visible light activated carbon and nitrogen co-doped mesoporous $TiO_2$ as efficient photocatalyst for degradation of ibuprofen. Separation and Purification Technology. 2017;**173**:258-268

[39] Benetti D, Dembele KT, Benavides J, Zhao H, Cloutier S, Concina I, Vomiero A, Rosei F. Functionalized multi-wall carbon nanotubes/$TiO_2$ composites as efficient photoanodes for dye sensitized solar cells. Journal of Materials Chemistry C. 2016;**4**:3555-3562

[40] Mutuma BK, Shao GN, Kim WD, Kim HT. Sol–gel synthesis of mesoporous anatase–brookite and anatase–brookite–rutile $TiO_2$ nanoparticles and their photocatalytic properties. Journal of Colloid and Interface Science. 2015;**442**:1-7

[41] Fakhouri H, Arefi-Khonsari F, Jaiswal AK, Pulpytel J. Enhanced visible light photoactivity and charge separation in $TiO_2$/TiN bilayer thin films. Applied Catalysis A: General. 2015;**492**:83-92

[42] Li X, Colombo L, Ruoff RS. Synthesis of Graphene films on copper foils by chemical vapor deposition. Advanced Materials. 2016;**28**:6247-6252

[43] Pierson HO. Handbook of Chemical Vapor Deposition (CVD)—Principles, Technology and Applications. 2nd Ed. Norwich, NY: William Andrew Publishing/Noyes; 1999

[44] Bento RT, Ferrus Filho A, Pillis MF. Microstructural characterization of $TiO_2$ thin films: A review. Revista Brasileira de Inovação Tecnológica em Saúde. 2017;**7**:4-17

[45] Marcello BA, Geribola GA, Pillis MF. Caracterização de filmes finos de $TiO_2$ crescidos sobre borossilicato. In: XXI Congresso Brasileiro de Engenharia e Ciência dos Materiais. Cuiabá: Proceedings of XXI CBECIMAT. Vol. 1. 2014. pp. 768-775

[46] Zhou M, Yu J, Liu S, Zhai P, Jiang L. Effects of calcination temperatures on photocatalytic activity of $SnO_2$/$TiO_2$ composite films prepared by an EPD method. Journal of Hazardous Materials. 2008;**154**:1141-1148

[47] Whitehouse DJ. Handbook of Surface Metrology. Vol. 988. London: IOP Publishing Ltd; 1994

[48] Krumdieck S, Gorthy R, Gardecka AJ, Lee D, Miya SS, Talwar SD, Polson MIJ, Bishop C. Characterization of photocatalytic, wetting and optical properties of $TiO_2$ thin films and demonstration of uniform coating on a 3-D surface in the mass transport controlled regime. Surface and Coatings Technology. 2017;**326**:402-410

[49] Antunes RA, Oliveira MCL, Pillis MF. Effect of the deposition temperature on the corrosion stability of $TiO_2$ films prepared by metal organic chemical vapor deposition. International Journal of Electrochemical Science. 2013;**8**:1487-1500

[50] Liu R, Zhou X, Yang F, Yu Y. Combination study of DFT calculation and experiment for photocatalytic properties of S-doped anatase $TiO_2$. Applied Surface Science. 2014;**319**:50-59

[51] Babelon P, Dequiedt AS, Mostéfa-Sba H, Bourgeois S, Sibillot P, Sacilott M. SEM and XPS studies of titanium dioxide thin films grown by MOCVD. Thin Solid Films. 1998;**332**:63-67

[52] Georgios P, Wolfgang SM. X-ray photoelectron spectroscopy of Anatase-TiO$_2$ coated carbon nanotubes. Solid State Phenomena. 2010;**162**:163-177

[53] Bharti B, Kumar S, Lee H-N, Kumar R. Formation of oxygen vacancies and Ti$^{3+}$ state in TiO$_2$ thin film and enhanced optical properties by air plasma treatment. Scientific Reports. 2016;**6**:32355

[54] Lin L, Wang H, Luo H, Xu P. Enhanced photocatalysis using side-glowing optical fibers coated with Fe-doped TiO$_2$ nanocomposite thin films. Journal of Photochemistry and Photobiology A: Chemistry. 2015;**307-308**:88-98

[55] Wang F, Li F, Zhang L, Zeng H, Sun Y, Zhang S, Xu X. S-TiO$_2$ with enhanced visible-light photocatalytic activity derived from TiS$_2$ in deionized water. Materials Research Bulletin. 2017;**87**:20-26

[56] Hu B, Liu Y. Nitrogen-doped Nb$_2$O$_5$ nanobelt quasi-arrays for visible light photocatalysis. Journal of Alloys and Compounds. 2015;**635**:1-4

[57] Mourão HAJL, De Mendonça VR, Malagutti AR, Ribeiro C. Nanostructures in photocatalysis: A review about synthesis strategies of photocatalysts in nanometric size. Química Nova. 2009;**32**:2181-2190